

# Ultrastructural Pathology of Paraquat (PQ) Induced Acute and Subacute Lung Injury in Experimental Rats

Mekala Lakshman<sup>1</sup>, Vallapureddy Sudha<sup>2</sup>, Bathula Haripriya<sup>3</sup>

<sup>1</sup>Professor & Officer-in-charge, Ruska Labs, Department of Veterinary Pathology, College of Veterinary Science, Rajendranagar, Hyderabad-30, India

<sup>2</sup>Veterinary Assistant Surgeon, Department of Animal Husbandry, Govt. of T.S. India

<sup>3</sup>Post Graduate Student in Biotechnology, SPMVV, Tirupati. A.P, India

**Abstract:** Paraquat (PQ) is a widely used herbicide throughout the globe, which induces acute lung injury (ALI) in rats. Studies on acute and subacute lung injury due to PQ toxicity at different doses through different routes are sparse. Microscopically (LM and EM) a noteworthy changes like proliferation of fibrous tissue into lung parenchyma and also in liver and mild to moderate changes kidney. Significant alterations in body weights and haematobiochemical parameters were also documented in acute (24, 48, 72 hrs) and subacute (7, 14, 21 days) study in male Wister rats.

**Keywords:** PQ, ALI, TEM and SEM

## 1. Introduction

Paraquat (1,1 dimethyl -4,4 bipyridinium) is most widely used quaternary ammonium quick acting, non selective herbicide in the world. PQ identified in 1955, and introduced commercially in 1962 [1]. PQ is highly toxic to human [3,4,5,6] and animals [7,8,9,10] leading to acute respiratory distress syndrome (ARDS) [2]. Occupational hazards of PQ in different developing countries were also documented [11]. In this context two experiments were carried out to study the haemato-biochemical alterations, light microscopy (LM) and electron microscopy (EM) of lung, liver and kidney in experimental rats.

## 2. Materials and Methods

Total 84 adult *Wister male albino rats* were used for two experiments after approval of Institutional Animal Ethics Committee (IAEC-GPRCP/IAEC/07/17/01/PCL/AE-3-Rats-M-84). All animals were weighed (180-240 g) on day one and marked individually for identification, reared under controlled temperature (22°C) and identical conditions. Standard pellet diet and deionized water was provided *ad libitum* throughout the experimental period. 1<sup>st</sup> experiment was carried out to study the acute lung injury (ALI) and 2<sup>nd</sup> experiment to study the subacute toxic effects on lung. In both experiments a single dose PQ was administered through intraperitoneal (I/P) and oral gavage. In addition to lung the toxic effects of PQ was also carried out in liver and kidney in both the experiments.

### 2.1. Experiment-I.

ALI was induced in first experimental rats by injecting PQ @24 mg/kg b.wt at different time intervals (24, 48 and 72 h) for which 36 rats were divided into control group (G1) and PQ treated group (G2), further subdivided into three sub groups (G2a, G2b and G2c) based on aforementioned time intervals. A day before sacrifice blood samples were

collected for haematobiochemical parameters. Respective tissue samples were collected and preserved in suitable fixatives and processed for Light Microscopy (LM) and Electron Microscopy (EM) as per the standard protocols [12, 13].

### 2.2 Experiment-II.

Second experiment was conducted for 21 days to study the subacute lung injury through oral gavage of PQ@ 40 mg/kg b.wt, and also to study the pomegranate seed extract (PSE) ameliorating effect against lung injury which was given through drinking water daily. 48 animals were divided into four groups 1<sup>st</sup> group was served as control, 2<sup>nd</sup> group was administered with PQ, 3<sup>rd</sup> group was provided with PSE and 4<sup>th</sup> group was treated with PQ and PSE. Similar to that of 1<sup>st</sup> experiment blood and tissue samples were collected on 7<sup>th</sup>, 14<sup>th</sup> and 21<sup>st</sup> day of experiment to study the haematobiochemical parameters LM and EM of respective tissue samples.

## 3. Results and Discussion

Clinically all PQ treated animals were inactive, reluctant to take feed and water, most of the animals started showing deep shallow abdominal breath after 24 hrs in first experiment and after 7<sup>th</sup> in second experiment. Animals showed redness of nostrils and eyes in both experiments after 48 hrs and 14<sup>th</sup> day respectively. Significant decrease in body weights was recorded among PQ treated rats of both the experiments which could be due to PQ induced toxic effects have made the animals disinclination towards feed and water [14,15,16]. Grossly edema, congestion, hemorrhages emphysema of lungs (Fig.1). Mild to moderate swelling of liver, petechial hemorrhages of liver and kidneys (Fig2&3) was noticed among both the experimental animals [15,21,22]. This could be due to PQ induced toxic action of congestion due to mild to moderate dilation of micro and macrocapillaries of respective organs.

Acute study lung specimens showed an increased thickness of septa and collapsed alveoli, mild to moderate hyperplasia of epithelial cells and focal areas inflammatory cells infiltration a dark inclusion like bodies and mild fibrous tissue proliferation, severe congestion in peribronchial area along with few shrunken bronchioles and few showing severe congestion tertiary bronchiole filled with blood mild fibrous tissue proliferation, infiltration of inflammatory cells and shrunken bronchioles (Fig. 4). Edema, emphysema diffuse haemorrhages, and focal areas of pneumonia was observed in subacute experiment [15,20,21]. Congestion of central vein, moderate to severe dilation of sinusoids with mild proliferation of Kupffer cells in liver (Fig. 5). Congestion, hemorrhages, degeneration of epithelial cells, with mild to moderate casts in tubules of kidneys (Fig. 6) were noticed in both the experiments under LM [15,16,17].

SEM revealed hemorrhagic irregular surface area with thickened alveolar septa and peribronchial fibrosis (Fig.7, 8, 9) among 48 and 72 hours specimens but not on 24 hours of first experiment and subacute study. TEM of PQ group lungs revealed vesicular cytoplasm, swollen to vesicular and electron dense mitochondria with loss of cristae and matrix (Fig. 10). Eccentrically placed swollen nucleus with indistinct nuclear membrane and increased perinuclear space in type I and type II pneumocytes. In the vicinity of type II pneumocytes number of dilated alveoli filled with blood, few pneumocytes showed stunted microvilli, elongated mitochondrion, desquamation of epithelial cells and blood filled dilated alveolar spaces, proliferation of fibroblasts around distorted pneumocytes and peribronchial area, entry of macrophage in to alveolar lumen was also noticed in majority sections (Fig. 11&12). These changes could be due to ROS induced mitochondrial dysfunction [15,21,23,24].

SEM of liver slices revealed (24 hrs) dilation and congestion of central vein with abundant number of altered erythrocytes on irregular surface area. At 48 hrs of experiment the cut surface of liver slices showed shrunken hepatic cords with mild proliferation of fibrous tissue and moderate dilation of sinusoids. Vacuolar degeneration of hepatocytes with mild hemorrhages and presence of few fat like globular structures in dilated areas were noticed. And at 72 hrs liver slices revealed zigzag shrunken cords with rough surface, mild hemorrhage, numerous fat like globules and mild proliferation of fibrous tissue (Fig. 13-15). TEM liver sections showed congestion of central vein, necrosis, altered parenchyma and mild fibrous tissue proliferation with numerous fat bodies observed in acute studies, additionally vesicular cytoplasm and condensed electron dense mitochondria, increased nuclear pores, increased perinuclear space, mild to moderate dilation of rough endoplasmic reticulum (RER), thick nuclear membrane and proliferation of few Kupfer cells was seen in subacute experiment (Fig. 16-18). This could be due to targeted toxic action of PQ on subcellular membranous strictures like mitochondrion of liver [15].

SEM (24 hrs) of kidney slices showed swollen glomeruli and mild hemorrhages, sections of 48 hrs revealed hemorrhages with an abnormal erythrocytes and leucocytes, whereas 72 hrs samples showed few swollen and few shrunken glomeruli (Fig. 18-21). TEM of kidney sections of PQ group of both experiments showed variation in shape and size of mitochondrion, in few section showed altered mitochondria arranged in rows in few shrunken podocytes with blunt foot process (Fig. 22-24) were observed.

#### 4. Figures:



Figure 1: Lung

Figure 2: Liver

Figure 3: Kidney

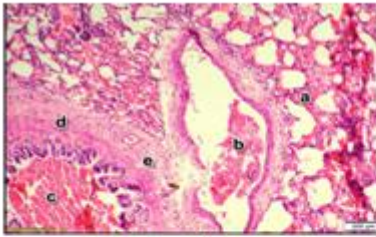


Figure 4 Lung

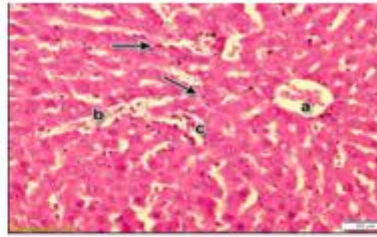


Figure 5 Liver

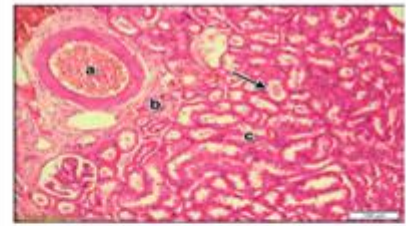


Figure 6 Kidney

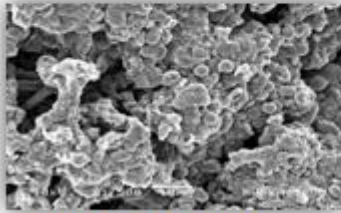


Figure 7 SEM Lung

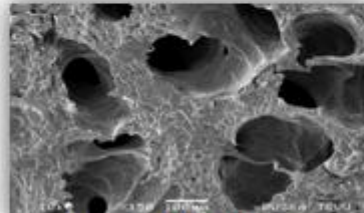


Figure 8 SEM Lung

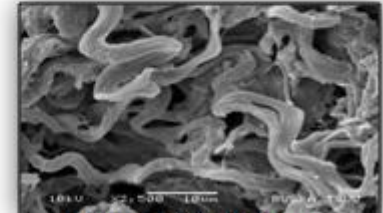


Figure 9 SEM Lung

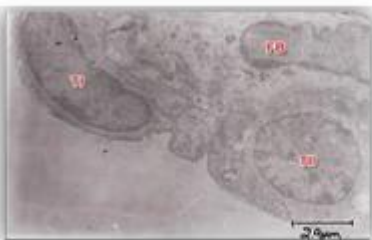


Figure 10 TEM Lung

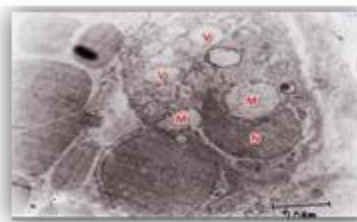


Figure 11 TEM Lung

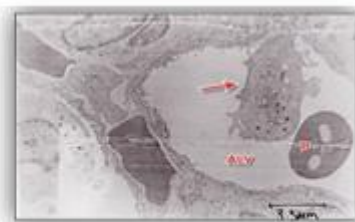


Figure 12 TEM Lung

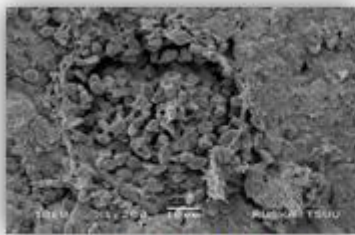


Figure 13: SEM Liver

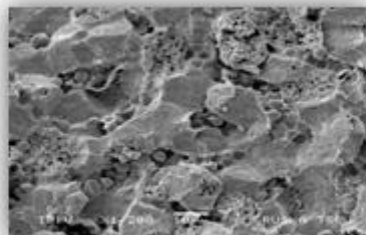


Figure 14: SEM Liver

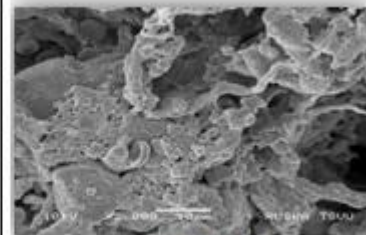


Figure 15: SEM Liver

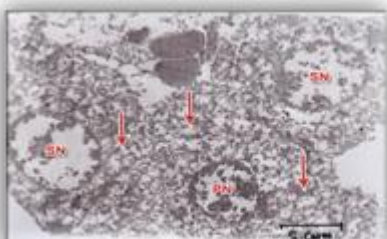


Figure 16: TEM Liver

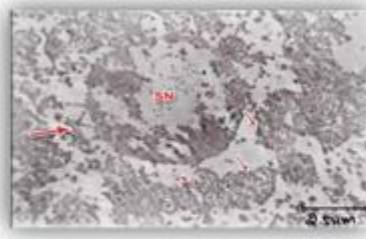


Figure 17: TEM Liver

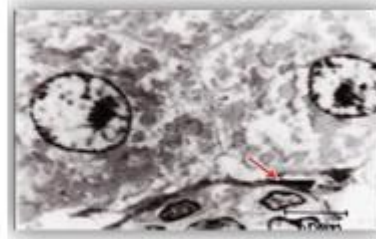


Figure 18: TEM Liver

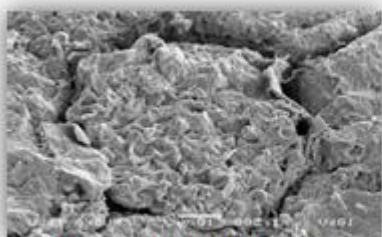


Figure 19 SEM Kidney

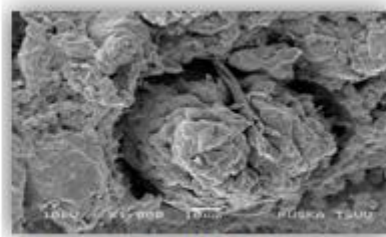


Figure 20 SEM Kidney

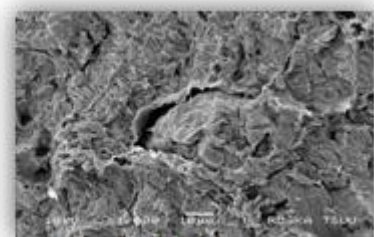
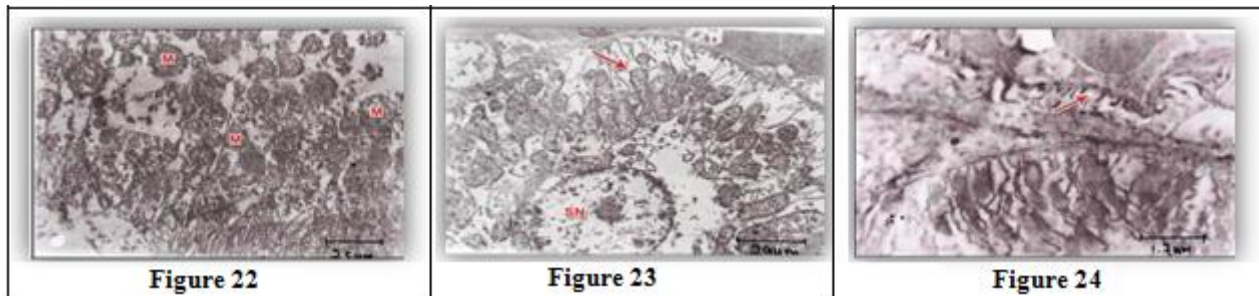


Figure 21 Kidney



**Figure**

Fig. 1 Lung showing edema, congestion, hemorrhages emphysema.

Fig. 2 Liver showing mild to moderate swelling and petechial hemorrhages.

Fig. 3 Kindney showing mild to moderate swelling and petechial hemorrhages.

Fig. 4 Photomicrograph of lung showing severe congestion teriory bronchiole filed with blood mild fibrous tissue proliferation, infiltrartion of inflammatoy cells and shrunken bronchioles. H&E,200µm.

Fig. 5 Photomicrograph of liver showing congestion of central vein, moderate to severe dilation of sinusoids with mild proliferation of Kupffer cells.H&E,50µm.

Fig. 6 Photomicrograph kidney showing thickened wall of blood vessel, congestion, degeneration of epithelial cells, with mild to moderate cats in tubules.H&E, 100µm.

Fig. 7 Scanning electron micrograph showing 24 hrs treated lung with hemorrhages in septa.

Fig. 8 Scanning electron micrograph showing 48 hrs treated lung with thickened alveolar septa.

Fig. 9 Scanning Electron Micrograph of lung of 48 and 72 hrs treated revealing lung hemorrhagic irregular surface area with thickened alveolar septa and peribrochial fibrosis.

Fig. 10 Transmission Electron Micrograph of lung revealing depecting vesicular cytoplasm, swollen to vesicular and electron dense mitochondria with loss of cristae and matrix. UA & LC, x9650.

Fig. 11 &12 Transmission Electron Micrographs of pneumocytes showing stunted microvilli, elongated mitochondrion, desquamation of epithelial cells and blood filled dilated alveolar spaces, proliferation of fibroblasts around distorted pneumocytes and peribrochial area entry of macrophage in to alveolar lumen was also evidenced. UA & LC, x5790 and x6755.

Fig. 13 Scanning Electron Micrograph showing 24 treated liver with congestion, dilation of central vein and erythrocytes.

Fig. 14 Scanning Electron Micrograph showing 48 hrs treated liver with shrunken hepatic cords, fibrous tissue,

moderate dilation of sinoviocytes and hepatocytes vacuulation.

Fig. 15 Scanning Electron Micrograph showing 72 hrs treated liver with numerous fat like globular structures and fibrous tissue proliferation.

Fig. 16 Transmission Electron Micrograph of liver showing altered parenchyma, vesicular mitochondrion (arrow)indistinct cell junctions, swollen nucleus (SN) and pyknotic nuclei (PN) with irregular margination of chromatin. UA & LC, x3860.

Fig. 17 Transmission Electron Micrograph of liver showing swollen nucleus (SN) abnormal chromatin, dilated nuclear pores incresed perinuclear space, electron dense granular mitochondria (samll arrow), condensed discontinous RER (long arrow) UA & LC, x7720.

Fig. 18 Transmission Electron Micrograph of liver showing distorted hepatocytes with thick nuclear membrane mild margination of chromatin and proliferating Kupffer cells (arrow). UA & LC, x3860.

Fig. 19-21 Scanning Electron Micrograph showing 24, 48 and 72 hrs treated kidney with swollen glomeruli and mild hemorrhages, distorted tubules and shrunken glomeruli.

Fig. 22 Transmission Electron Micrograph of PCT showing variation in shape and size of mitochondria with electron dense cristae and matrix (M). UA & LC, x7720.

Fig. 23 Transmission electron micrograph of renal tubules showing distorted mitochondrion arranged in rows (arrow) and swollen nucleus (SN) UA & LC, x6755.

Fig. 24. Transmission Electron Micrograph of glomerular membrane showing shrunken podocytes with blunt foot process (arrow) with thin Bowmans' capsule.UA & LC, x11580.

**References**

- [1] Revkin, A. C. "Paraquat: A potent weed killer is killing people". Science Digest, 91 (6) (1983) 36–38.
- [2] Huang CJ, Yang MC and Ueng SH: Subacute pulmonary manifestation in a survivor of severe paraquat intoxication. Am J Med Sci. 330 (2005) 254-256.
- [3] J.S.Sandhu, A.Dhiman, R.Mahajan and P.Sandhu. Outcome of paraquat poisoning - a five year study. Indian J. Nephrol. 13 (2003) 64-68.

- [4] Surendra Khosya<sup>2</sup> and Sunil Gothwal. Two Cases of Paraquat Poisoning from Kota, Rajasthan, India, *Case Reports in Critical Care*. (2012) 1-3.
- [5] Kavitha Saravu, Sonal Sekhar, Ananth Pai, Ananthakrishna Shastry Barkur, V. Rajesh and Jagadeswara Rao Earla, Paraquat - A deadly poison: Report of a case and review, *Indian J. of Critical Care Medicine*. 17(3) (2013) 182-184.
- [6] Narendra S. S, and S Vinaykumar, Paraquat Poisoning: A Case Series in South India, *Intern.J.of Science and Research*. (2013) 561-564.
- [7] R.B. Cope, Helping animals exposed to the herbicide paraquat, *Veterinary Medicine* 2004 (Sept) 755-760.
- [8] June H. Williams, Zandri Whitehead, Erna van Wilpe, Paraquat intoxication and associated pathological findings in three dogs in South Africa, *J. of the South African Veterinary Assoc.* (2016) 1-9.
- [9] G. S, Vijayarathnam and B Corrin, Experimental paraquat poisoning: a histological and electron-optical study of the Changes in the lung, *J. Path.* 103 (1971) 123-129.
- [10] M.F.R Silva, and P.H.N Saldiva, Paraquat poisoning: an experimental model of dose-dependent acute lung injury due to surfactant dysfunction, *Braz. J. Med. Biol. Res.* 31(3) (1998) 4454-450.
- [11] Catharina Wesseling, Berna van Wendel De Joode, Clemens Ruppert, Catalina León, Patricia Monge, Hernán Hermosillo and Timo J. Partanen, Paraquat in Developing Countries, *Int. J. Occup. Environ. Health*. 7 (2001) 275-286.
- [12] Luna G. L. H. T. *Manual of histological and special staining techniques*. Second ed., The Blakistone Division McGraw-Hill Book Company, Inc. New York, Toronto London: 1968. pp.1-5 and 9-34.
- [13] John J. Bozzola, and Lonnie D. Russell, *Electron Microscopy Principles and Techniques for Biologists* second ed., Jones and Bartlett Publishers, Sudbury, Massachusetts. 1998. pp. 19 to 45 and 72 to 144.
- [14] Igarashi, K., Kimura, Y. and Takenaka, A. 2000. Preventive effects of dietary cabbage acylated anthocyanins on paraquat-induced oxidative stress in rats. *Bioscience, biotechnology and biochemistry* **64** (8): 1600-1607.
- [15] Dinis-Oliveira, R. J., De Jesús, V. M., Bastos, M. L., Carvalho, F. and Sánchez, N. A. 2006. Kinetics of paraquat in the isolated rat lung: Influence of sodium depletion. *Xenobiotica; the fate of foreign compounds in biological systems* **36** (8): 724-737.
- [16] Lalruatfela, P. L., Saminathan, M., Ingole, R. S., Dhama, K. and Joshi, M. V. 2014. Toxicopathology of paraquat herbicide in female wistar rats. *Asian Journal of Animal and Veterinary Advances* **9**: 523-542.
- [17] Akinloye, O.A., Adamson, I. and Arowolo, T.A., 2011. Supplementation of vitamins C, E and its combination on paraquat-intoxicated rats: effects on some biochemical and markers of oxidative stress parameters. *Journal of Applied Pharmaceutical Science* **1** (6): 85-91.
- [18] Attia, A. M. and Nasr, H. M., 2009. Evaluation of protective effect of omega-3 fatty acids and selenium on paraquat intoxicated rats. *Slovak J Anim Sci* **42**: 180-187.
- [19] Ahmad, I., Shukla, S., Kumar, A., Singh, B.K., Kumar, V., Chauhan, A. K., Singh, D., Pandey, H.P. and Singh, C. 2013. Biochemical and molecular mechanisms of N-acetyl cysteine and silymarin-mediated protection against maneb-and paraquat-induced hepatotoxicity in rats. *Chemico-biological interactions* **201** (1): 9-18.
- [20] Ghazi-Khansari, M., Mohammadi-Karakani, A., Sotoudeh, M., Mokhtary, P., Pour-Esmail, E. and Maghsoud, S. 2007. Antifibrotic effect of captopril and enalapril on paraquat-induced lung fibrosis in rats. *Journal of Applied Toxicology* **27** (4): 342-349.
- [21] Chang, X., Shao, C., Wu, Q., Huang, M. and Zhou, Z., 2009. Pyrrolidinedithiocarbamate attenuates paraquat-induced lung injury in rats. *Bio Med Research International*: 1-8.
- [22] Zhang, Z., Ding, L., Wu, L., Xu, L., Zheng, L. and Huang, X. 2014. Salidroside alleviates paraquat-induced rat acute lung injury by repressing TGF- $\beta$ 1 expression. *International journal of clinical and experimental pathology* **7** (12): 8841.
- [23] Smith, P. and Heath, D. 1974. The ultrastructure and time sequence of the early stages of paraquat lung in rats. *Journal of Pathology* **114** (4): 177-184.
- [24] Fukushima, T., Yamada, K., Isobe, A., Shiwaku, K. and Yamane, Y. 1993. Mechanism of cytotoxicity of paraquat: I. NADH oxidation and paraquat radical formation via complex I. *Experimental and Toxicologic Pathology* **45**(5-6): 345-349.